tvst

Article

Progression of cRORA (Complete RPE and Outer Retinal Atrophy) in Dry Age-Related Macular Degeneration Measured Using SD-OCT

Or Shmueli[1], Roei Yehuda[2], Adi Szeskin[2], Leo Joskowicz[2], and Jaime Levy[1]

[1] Department of Ophthalmology, Hadassah-Hebrew University Medical Center, Jerusalem, Israel
[2] School of Computer Science and Engineering, The Hebrew University of Jerusalem, Givat Ram, Jerusalem, Israel

Correspondence: Jaime Levy, Ophthalmology Department, Hadassah Medical Center, The Hebrew University of Jerusalem, Ein-Karem 91120, Israel.
e-mail: levjaime@gmail.com

Received: August 3, 2021
Accepted: December 17, 2021
Published: January 14, 2022

Keywords: age-related macular degeneration; complete retinal pigment epithelium (RPE) and outer retinal atrophy; OCT scan analysis; retinal atrophy progression

Citation: Shmueli O, Yehuda R, Szeskin A, Joskowicz L, Levy J. Progression of cRORA (complete RPE and outer retinal atrophy) in dry age-related macular degeneration measured using SD-OCT. Transl Vis Sci Technol. 2022;11(1):19, https://doi.org/10.1167/tvst.11.1.19

Purpose: The purpose of this study was to evaluate the long-term rate of progression and baseline predictors of geographic atrophy (GA) using complete retinal pigment epithelium and outer retinal atrophy (cRORA) annotation criteria.

Methods: This is a retrospective study. Columns of GA were manually annotated by two graders using a self-developed software on optical coherence tomography (OCT) B-scans and projected onto the infrared images. The primary outcomes were: (1) rate of area progression, (2) rate of square root area progression, and (3) rate of radial progression towards the fovea. The effects of 11 additional baseline predictors on the primary outcomes were analyzed: total area, focality (defined as the number of lesions whose area is >0.05 mm^2), circularity, total lesion perimeter, minimum diameter, maximum diameter, minimum distance from the center, sex, age, presence/absence of hypertension, and lens status.

Results: GA was annotated in 33 pairs of baseline and follow-up OCT scans from 33 eyes of 18 patients with dry age-related macular degeneration (AMD) followed for at least 6 months. The mean rate of area progression was 1.49 ± 0.86 mm^2/year ($P < 0.0001$ vs. baseline), and the mean rate of square root area progression was 0.33 ± 0.15 mm/year ($P < 0.0001$ vs. baseline). The mean rate of radial progression toward the fovea was 0.07 ± 0.11 mm/year. A multiple variable linear regression model (adjusted $r^2 = 0.522$) revealed that baseline focality and female sex were significantly correlated with the rate of GA area progression.

Conclusions: GA area progression was quantified using OCT as an alternative to conventional measurements performed on fundus autofluorescence images. Baseline focality correlated with GA area progression rate and lesion's minimal distance from the center correlated with GA radial progression rate toward the center. These may be important markers for the assessment of GA activity.

Translational Relevance: Advanced method linking specific retinal micro-anatomy to GA area progression analysis.

Introduction

Geographic atrophy (GA) is a major cause of vision loss secondary to age-related macular degeneration (AMD) that currently has no treatment.[1] Several traditional and recently developed imaging technologies can be used to quantify morphological signs of atrophy in the setting of AMD, including color fundus photography (CFP), fundus autofluorescence (FAF), infrared imaging (IR), and spectral-domain optical coherence tomography (SD-OCT; hereafter referred to as OCT). The earliest diagnosis can be obtained using OCT imaging, as reported in a recent consensus paper by retinal specialists worldwide.[2] Specifically, these specialists proposed a classification system that includes incomplete retinal pigment epithelium (RPE) and outer retinal atrophy (iRORA) and complete RPE and outer

retinal atrophy (cRORA), with increasing levels of severity. The cRORA is defined as the complete loss of photoreceptors and the RPE, providing a specific anatomical measure of GA that will likely be critical for clinical trials designed to prevent atrophy; importantly, cRORA can be detected only on OCT, but not on FAF or CFP.[2]

Most studies that address the rate of GA progression are based on CFP or FAF. A meta-analysis by Fleckenstein et al. found that a median rate of GA progression of 1.78 mm^2 /year.[1] Multifocality of baseline GA lesions has been shown to correlate with faster GA area progression rate.[3] In addition, baseline foveal sparing has been associated with increased overall radial progression of atrophy.[4]

In previous work, we developed a custom image analysis software platform for measuring GA progression in OCT scans using cRORA criteria for GA annotation.[5] Here, we used this system to annotate and quantify the rate of GA progression in patients with GA secondary to AMD and to identify potential baseline predictors of GA progression.

Methods

Study Design, Patient Selection, and Data Collection

In this retrospective study, we collected the baseline and follow-up data of eyes with advanced dry AMD in patients who were followed during the years 2012 to 2020 at the Retina Service of the Department of Ophthalmology at the Hadassah-Hebrew University Medical Center in Jerusalem, Israel. This study was performed in accordance with the Declaration of Helsinki and was approved by our Institutional Review Board (IRB)/Ethics Committee (approval number HMO-382-19). Informed consent was not required due to the retrospective study design and anonymous data analysis.

We included patients over 55 years of age who presented with GA secondary to AMD on OCT and were followed for at least 6 months. Additional inclusion criteria included no signs or history of choroidal neovascularization on fundoscopy or OCT in the study eye(s) and suitable quality baseline and follow-up images (defined subjectively by the graders as a high signal-to-noise ratio, to prevent interfering with proper annotation). We excluded patients with retinal atrophy due to high myopia (spherical equivalent >6 diopters) and/or macular dystrophy, as well as patients with occluded ocular media (e.g. due to dense cataracts or corneal scarring).

Patients underwent best-corrected visual acuity (BCVA) testing (early treatment diabetic retinopathy study [ETDRS] protocol at a distance of 4 meters), slit-lamp examination, bio-microscopy, and OCT with simultaneous infrared imaging (Spectralis OCT system; Heidelberg Engineering GmbH, Heidelberg, Germany). Patient demographics (e.g. sex and age) and lens status (i.e. pseudophakia) were extracted from the patients' electronic medical records.

Retinal Imaging Protocol

The Spectralis HRA-OCT protocol includes 25 to 61 B-scan slices per cube scan (baseline and follow-up; 20 pairs had 61 B-scans per cube scan, 5 pairs had 49 B-scans per cube scan, 3 pairs had 37 B-scans per cube scan, and 5 pairs had 25 B-scans per cube scan), with a width and height of 20 degrees in each direction. Different patients had different numbers of slices; however, the same number of slices was used for the baseline and follow-up scans in each patient. Each scan was averaged using the automated real-time mode of the Spectralis system, with 30 frames per B-scan. The confocal scanning-laser ophthalmoscopy device for infrared imaging in the Spectralis HRA-OCT system uses a wavelength of 820 nm. Infrared images were acquired simultaneously during the OCT procedure with a frame size of 30 degrees × 30 degrees and a resolution of 768 × 768 pixels. The technical properties of the infrared and OCT images and of the procedures used are described elsewhere.[6]

Image Analysis and Annotation

Columns of GA lesions were manually annotated in 66 cube scans by 2 experienced graders (authors J.L. and O.S.); 52 scans were annotated by one grader and validated by the second grader, whereas the remaining 14 scans were independently annotated by the second grader. Lesion size was calculated as the average of the two annotations made by the graders where appropriate. Our custom software program was used to manually annotate GA in the baseline and follow-up OCT B-scans.[5]

The "Consensus Definition for Atrophy Associated with Age-Related Macular Degeneration on OCT" (CAM) criteria for cRORA were used to annotate GA.[2] Columns of cRORA were annotated on each B-scan if all four of the following criteria for complete RPE and outer retinal atrophy (cRORA) were met: (1) choroidal hyper-transmission, (2) RPE attenuation or disruption, (3) evidence of overlying photoreceptor degeneration, and (4) absence of scrolled RPE or other signs of an RPE tear. However, unlike the CAM

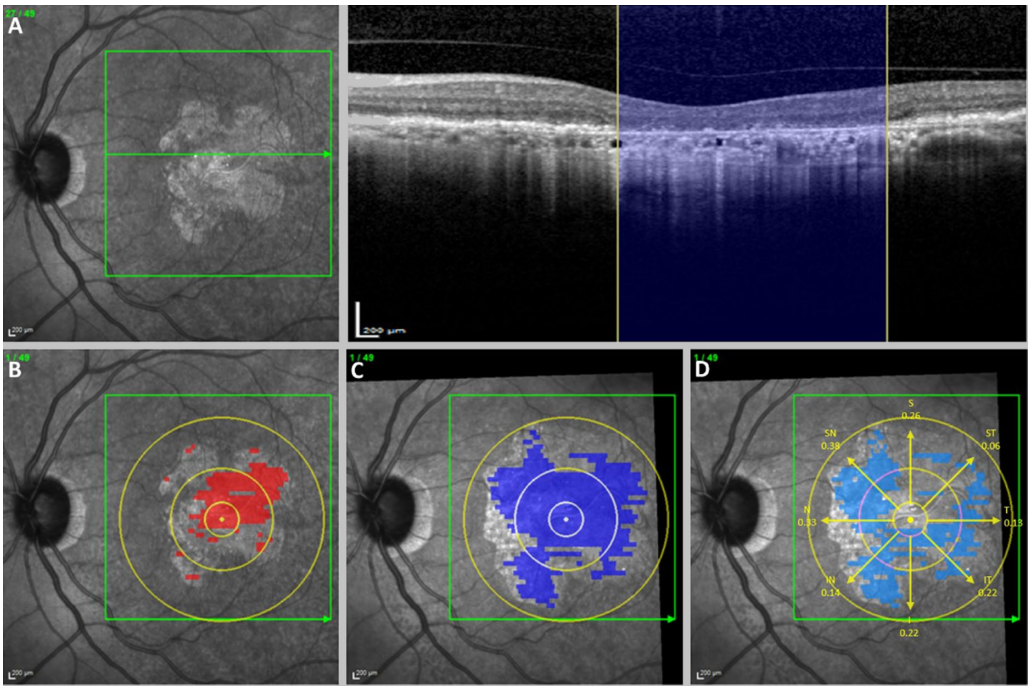

Figure 1. Annotation of GA using OCT scans. GA segments were annotated on OCT B-scans based on the presence of three specific criteria of cRORA: (1) choroidal hyper-transmission; (2) RPE attenuation or disruption; and (3) photoreceptor degeneration, which manifests as an absence of interdigitation zone, ellipsoid zone, and external limiting membrane, as well as thinning of the outer nuclear layer. Shown is an example of GA annotation at baseline using the cRORA criteria on an OCT B-scan (**A**) and the projection on the corresponding infrared image (**B, C, D**). The difference between the baseline **B** and follow-up **C** scans was used to calculate the rate of GA area progression and the rate of radial progression indicated the *yellow radial arrows* in **D**. *Red color* = GA annotation using the cRORA criteria on an OCT B-scan projected on the IR image on baseline; *dark blue color* = GA annotation using the cRORA criteria on an OCT B-scan projected on the IR image on follow-up; *light blue color* = annotation of GA progression on the follow-up scan relative to baseline; *yellow circles* = 1, 3, and 6-mm diameter distances from the foveal center (ETDRS grid); *yellow arrow* = radial progression in 8 radially equidistant directions at 45-degree intervals.

definition—and because of the technical capabilities of our custom image analysis program—we did not use the minimum diameter criteria of 250 microns; rather, we annotated lesions of any diameter greater than 200 microns provided they met the above-mentioned cRORA criteria.

Our image analysis software was performed by the graders for the manual annotation of GA columns in OCT B-scans. These manually annotated columns were then automatically aggregated by the software to form GA segments. Note that there can be more than one GA segment per OCT slice (i.e. OCT B-scan). The GA segments are then projected onto the corresponding IR image to form GA lesions (Fig. 1).

Figure 2 shows an example of a comparison of GA annotation with OCT using cRORA criteria, FAF and CFP. Note that the areas in this single comparison of GA annotation by cRORA criteria on OCT B-scan versus FAF are close in magnitude but not equal.

Next, the software was used to automatically compute the lesion area and the shape descriptive features (e.g. focality, circularity, perimeter, diameter, and distance of lesion from the center [see next section]).

To prevent over-annotation of lesions not related to AMD, the experts did not annotate any peripapillary atrophic lesions, defined as atrophy surrounding the disc and not connected to the macular GA. In areas in which there is a connection, the radius of the peripapillary atrophy was determined using the first point of disconnect from macular GA.

We compared the baseline and follow-up scans (Fig. 3) using the software program's registration function, which spatially aligns consistent topographic ocular features present on both scans. Our software was used to localize the foveal center and surround it with an overlay of an ETDRS grid in each scan.

Measured Parameters

In this study, we measured GA progression and shape-descriptive parameters with the self-developed

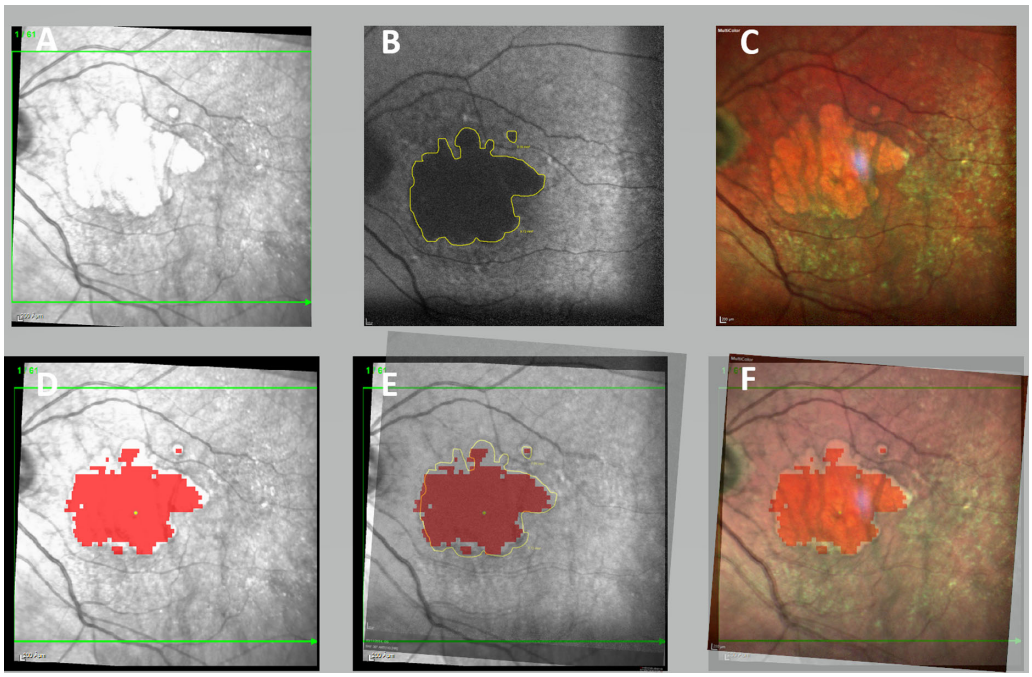

Figure 2. Annotation of GA using the cRORA criteria projected on IR-OCT compared to GA annotation on FAF and CFP. The first row shows (**A**) an IR image, (**B**) the corresponding GA annotation on FAF scan, and (**C**) the corresponding CFP scan. The second row shows (**D**) GA annotation using the cRORA criteria on an OCT B-scan projected on the IR image, (**E**) aligned with the annotated FAF scan, and (**F**) aligned with the CFP. The measured area of the manual annotation of the GA in the FAF scan is 9.82 mm^2. The measured area of the manual annotation of the GA using the cRORA criteria on the IR-OCT scans is 9.33 mm^2. The areas in this single comparison of GA annotation by cRORA criteria on OCT B-scan versus FAF are close in magnitude but not equal. IR-OCT = infra-red optical coherence tomography scan; FAF = fundus autofluorescence; CFP = color fundus image.

software. The majority of these parameters were assessed previously in the context of GA using FAF,[7,8] CFP,[9] or—less frequently—OCT.[10]

The GA area was measured 1, 3, and 6 mm from the foveal center, with the 1- and 3-mm diameter included in the 6-mm diameter area. These topographic markers correspond to the overlay of the ETDRS grid present in most OCT scans and have been used previously to study the area of retinal atrophy using OCT scans.[10]

As reported previously for FAF scans,[8] we also measured four additional baseline shape-descriptive factors: minimum and maximum lesion diameters (referred to as $Feret_{min}$ and $Feret_{max}$, respectively); focality index (defined as the number of lesions with an area >0.05 mm^2); and circularity index defined as $4\pi \times (\text{area}/\text{perimeter}^2)$.

Finally, we also measured the total baseline lesion perimeter,[3] as well as the minimum lesion distance from the fovea. In total, 14 measures were computed for each study.

Study Outcomes

The three primary outcomes of this study were: (1) the rate of GA area progression (measured in mm^2/year); (2) the rate of GA square root area progression (measured in mm/year); and (3) the rate of radial progression toward the fovea (measured in mm/year). As a secondary outcome, we also measured the difference in radial progression in 8 radially equidistant directions at 45-degree intervals. We also analyzed the putative effects of various baseline factors on the primary outcomes. These baseline factors included the total lesion area, focality, circularity, total lesion perimeter, $Feret_{min}$, $Feret_{max}$, the minimum distance from the center, sex, age, presence of hypertension, and lens status (pseudophakia).

Statistical Analysis

Differences in the primary outcome measurements between baseline and follow-up were analyzed using the paired Student's *t*-test. In addition, we first tested the effects of potential baseline factors on the primary outcome measures using univariate regression analysis. Subsequently, additional factors that had a significant effect on any of the primary outcome measures in the univariate analysis were included in a multivariate stepwise linear regression analysis. The

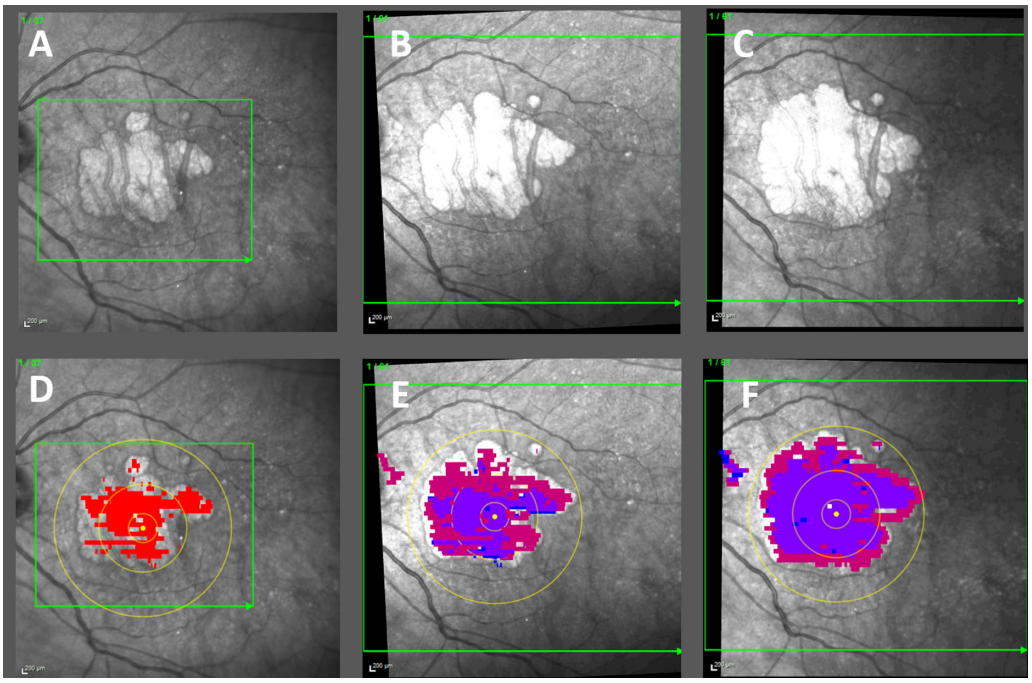

Figure 3. A series of annotated GA using the cRORA criteria on IR-OCT showing GA progression. Shown in the first row is an example of a baseline IR image (2013); (**A**) and two follow-up IR images (2015 and 2018; **B** and **C**, respectively). shown in the second row is the projection of the annotated GA using the cRORA criteria on the baseline (**D**), the progression of GA from baseline to follow-up one (**E**) and the progression of GA from follow-up one to follow-up two (**F**). The GA area was 5.36 mm^2 in 2013 (baseline), 11.63 mm^2 on 2015 (follow-up 1) and 17.17 mm^2 in 2018 (follow-up 2). *Red* color = GA annotation using the cRORA criteria on an OCT B-scan projected on the IR image on baseline; *purple* color = the overlapping annotation between current and previous scan; *magenta* color = annotation of GA progression on the current scan; *blue* color = GA area annotated on the previous but not the current scan. May represent the interobserver variability; *yellow circles* = 1, 3, and 6-mm diameter distances from the foveal center (ETDRS grid).

difference in radial progression in 8 radially equidistant directions at 45-degree intervals was compared using the Kruskal-Wallis test. The data were analyzed using SPSS software version 26 (IBM).

Results

A total of 33 pairs of baseline and follow-up OCT cube scans from 33 eyes of 18 patients with dry AMD were included in our analysis. Table 1 summarizes the baseline demographics. The mean follow-up time was 24.7 months (range = 7–59 months). Intergrader variability was measured using a dataset containing 612 standalone OCT slices from this study, and the resulting mean (±SD) dice coefficient was 0.73 ± 0.17, indicating a moderate degree of intergrader variability.

Rate of GA Area Progression

Table 2 shows the GA atrophy outcome measures for pairs of OCT scans of 33 eyes from 18 patients.

Table 1. Baseline Demographics of the Eyes Included in This Study ($N = 33$ Eyes From 18 Patients)

Parameter	Value
Left eyes/right eyes	
Left eyes	16 (48.5%)
Right eyes	17 (51.5%)
Follow-up, months	24.69 ± 14.05 (range = 7–59)
Age, years	77.87 ± 8.06 (range = 62–88)
Sex	
Male	17 (51.5%)
Female	16 (48.5%)
Pseudophakia	9 (39.1%)[a]
Hypertension	21 (63.6%)

Note: Data are presented as the mean ± standard deviation and range, or as *N* (%).

[a]Data were available for 23 eyes.

The total GA area increased significantly from 4.25 ± 2.77 mm^2 at baseline to 7.14 ± 4.14 mm^2 at the end of follow-up, with an annual progression rate of 1.49 ± 0.86 mm^2/year.

Table 2. Geographic Atrophy Outcome Measures ($N = 33$ Eyes From 18 Patients)

Factor	Baseline	Follow-Up	Yearly Progression	*P* Value
Total area, mm^2	4.25 ± 2.77 (0; 9.28)	7.14 ± 4.14 (0.04; 14.76)	1.49 ± 0.86 (0.03; 3.36)	**<0.0001**
1 mm diam. area, mm^2	0.28 ± 0.29 (0; 0.78)	0.35 ± 0.30 (0; 0.78)	0.04 ± 0.06 (0; 0.21)	**0.0025**
3 mm diam. area, mm^2	2.07 ± 1.70 (0; 5.97)	3.04 ± 1.96 (0.04; 6.61)	0.49 ± 0.38 (0.01; 1.38)	**<0.0001**
6 mm diam. area, mm^2	3.87 ± 2.64 (0; 8.57)	6.29 ± 3.76 (0.04; 14.76)	1.22 ± 0.69 (0.03; 2.57)	**<0.0001**
Total sq. rt. area, mm	1.87 ± 0.87 (0; 3.05)	2.50 ± 0.96 (0.20; 3.84)	0.33 ± 0.15 (0.07; 0.70)	**<0.0001**
1 mm diam. sq. rt. area, mm	0.405 ± 0.34 (0; 0.88)	0.50 ± 0.32 (0; 0.88)	0.06 ± 0.08 (0; 0.29)	**0.0007**
3 mm diam. sq. rt. area, mm	1.26 ± 0.70 (0; 2.44)	1.61 ± 0.66 (0.2; 2.57)	0.19 ± 0.16 (0.01; 0.83)	**<0.0001**
6 mm diam. sq. rt. area, mm	1.77 ± 0.86 (0; 2.93)	2.34 ± 0.90 (0.2; 3.84)	0.30 ± 0.18 (0.05; 0.99)	**<0.0001**
Perimeter, mm	24.34 ± 15.2 (0; 52.06)	33.73 ± 19.11 (0.58; 85.22)	4.40 ± 1.83 (0.27; 15.56)	**<0.0001**
Focality	5.41 ± 4.04 (0; 15)	5.82 ± 4.42 (0.5; 16.5)	0.20 ± 0.32 (0.30; 0.86)	**0.31**
Circularity	0.14 ± 0.13 (0.03; 0.58)	0.12 ± 0.11 (0.02; 0.43)	−0.01 ± 0.01 (−0.01; −0.03)	**0.22**
$Feret_{max}$, mm	4.95 ± 1.93 (0.5; 7.97)	5.47 ± 1.96 (0.62; 8.72)	0.79 ± 1.85 (0.2; 8.15)	**0.0005**
$Feret_{min}$, mm	3.44 ± 1.43 (0.3; 6.36)	4.11 ± 1.51 (0.52; 6.71)	0.84 ± 1.77 (0.1; 8.13)	**<0.0001**
Minimum distance from center, mm	0.28 ± 0.35 (0; 1.23)	0.18 ± 0.25 (0; 0.87)	−0.05 ± 0.08 (−0.07; 0)	**0.0040**

diam. = diameter; sq. rt = square root.

Table 3. Univariate Regression Analysis of Baseline Variables That Affect the Rate of GA Progression

		GA Area Progression Rate		GA Square Root Area Progression Rate		GA Radial Growth Rate Toward the Center	
Variable	*N*	r[a]	*P* Value	r[a]	*P* Value	r[a]	*P* Value
Total lesion[b] area	33	0.56	**0.0006**	–	–	0.10	0.57
Total lesion square root area[b]	33	–	–	0.09	0.60	0.03	0.86
Focality	33	0.74	**<0.0001**	0.51	**0.0023**	0.01	0.99
Circularity	33	−0.62	**0.0002**	−0.38	**0.036**	−0.15	0.42
Total lesion perimeter	33	0.76	**<0.0001**	0.32	0.069	0.04	0.84
$Feret_{max}$	33	0.65	**<0.0001**	0.13	0.48	0.04	0.82
$Feret_{min}$	33	0.66	**<0.0001**	0.18	0.32	0.06	0.79
Minimum distance from center	33	0.01	0.94	0.14	0.44	0.74	**<0.0001**
Female sex	33	0.36	**0.038**	0.29	0.09	0.37	**0.033**
Hypertension	33	−0.21	0.24	0.09	0.59	0.05	0.79
Pseudophakia	23	0.33	0.12	0.38	0.07	0.35	0.10
Age	33	0.06	0.72	0.20	0.25	0.13	0.45

Data are presented as the mean ± standard deviation (range).

[a]Pearson correlation coefficient.

[b]Baseline area and baseline square root area were used for the univariate regression analysis of GA area progression rate and square root area progression rate, respectively.

Table 3 shows the results of the univariate regression analysis. It revealed a significant correlation among the rate of GA area progression and the following variables: total area at baseline, baseline focality, baseline circularity, baseline perimeter, baseline $Feret_{max}$, baseline $Feret_{min}$, and female sex.

These seven variables were analyzed in a stepwise multivariate linear regression model. The multivariate model had an adjusted r^2 value of 0.522, and only baseline focality and female sex were significantly associated with the rate of GA area progression (Table 4).

Rate of GA Square Root Area Progression

We found that the total square root area of GA increased significantly from 1.87 ± 0.87 mm^2 at baseline to 2.50 ± 0.96 mm^2 at follow-up, with a progression rate of 0.33 ± 0.15 mm/year (see Table 2). Moreover, a univariate regression analysis revealed a significant correlation between the rate of GA square root area progression and both baseline focality and baseline circularity (see Table 3); however, neither of these variables was significantly associated with the rate of GA square root area progression in a multivariate model (see Table 4).

Table 4. Multivariate Regression Analysis of Baseline Variables Affecting the Rate of GA Progression

	GA Areaprogression Rate		GA Square Root Area Progression Rate		GA Linear Progression Toward the Center	
Variable	Estimated β	*P* Value	Estimated β	*P* Value	Estimated β	*P* Value
Total lesion area	0.176	**0.221**	NA	NA	NA	NA
Baseline focality	0.138	**<0.0001**	0.018	0.09	NA[a]	NA
Baseline circularity	−1.11	0.552	−0.125	0.585	NA	NA
Total lesion perimeter	0.299	0.201	NA	NA	NA	NA
$Feret_{max}$	0.182	0.390	NA	NA	NA	NA
$Feret_{min}$	0.226	0.258	NA	NA	NA	NA
Baseline minimum distance from center	NA	NA	NA	NA	0.259	**<0.0001**
Female sex	0.419	**0.045**	NA	NA	0.175	0.180
Adjusted r^2	**0.522**		0.184		**0.530**	

Variables that demonstrated a significant effect on either of the outcome measures in the univariate analysis were included in the multivariate analysis using stepwise linear regression.

[a]NA = not analyzed in the multivariate regression due to lack of a significant correlation on univariate regression analysis (see Table 3).

Rate of Radial GA Growth Toward the Center

The mean rate of radial GA growth toward the center was 0.07 ± 0.11 mm/year. Univariate regression analysis revealed a significant correlation between the rate of radial GA growth toward the center and both the baseline minimum distance from the center and female sex (see Table 3). Moreover, the multivariate model had an adjusted r^2 value of 0.530 and revealed that only the baseline minimum distance from the center was significantly associated with the rate of radial GA growth towards the center (see Table 4).

Growth in 8 Radially Equidistant Directions at 45-degree Intervals Relative to the Center

The rates of radial progression in 8 radially equidistant directions at 45-degree intervals were not statistically different from each other ($P = 0.09$). However, the most noticeable direction of GA growth was toward inferior, infero-temporal, temporal, and supero-temporal fields, which might be of interest for future studies using more subjects.

Index Case Demonstrating Annotation of GA Growth on Three Sequential Dates

Figure 3 shows a case of GA is that is analyzed to demonstrate the change in GA area annotation using cRORA criteria for two follow-up points. The annotation was performed as described above. The GA area was 5.36 mm^2 on 2013 (baseline), 11.63 mm^2 on 2015 (follow-up 1), and 17.17 mm^2 on 2018 (follow-up 2).

Discussion

Here, we quantitatively analyzed the progression of GA in patients with dry AMD using OCT scans and the criteria for cRORA based on the latest system for classifying atrophy.[10] We found that the progression of the GA area was correlated with baseline focality on multivariate analysis. Moreover, radial progression was correlated with the minimum distance between the lesion and the center at baseline on multivariate analysis.

Previous studies using CFP and/or FAF found that the rate of GA progression ranged from 0.534 to 2.642 mm^2/year, with a median rate of 1.78 mm^2/year.[1] In a recent meta-analysis by Shen et al., over 3000 eyes were imaged, most of them using FAF and CFP. Shen et al. reported a mean GA area progression ranging from 1.499 mm^2/year when involving the macular center to 1.995 mm^2/year when sparing the center.[7]

Other reports[4,10] on GA annotation on OCT scans found GA progression between 1.42 and 2.11 mm^2/year. However, the latest, updated OCT consensus classification system[11] was not used. In another study, atrophy—although not specifically cRORA—measured using OCT scans of 48 eyes yielded a mean rate of 2.11 mm^2/year.[12]

In our study, we measured a mean rate of area progression of 1.49 ± 0.86 mm^2/year, which is within

the range mentioned above but slightly lower than the median value reported by Fleckenstein et al.[1] This small difference could be due in part to the more specific and less sensitive end point of atrophy used in our study—namely, cRORA—compared to the more general forms of retinal atrophy measured with CFP, FAF, and even OCT when cRORA is not used as the outcome.

Moreover, this slightly slower GA progression measured on OCT B-scans as compared to FAF may be explained by the report of RPE dysmorphia surrounding GA on histology of retina from donor eyes.[13] RPE dysmorphia alone may allow for light to penetrate through RPE and manifest as hyper-autofluorescence.[14] However, it does not fulfill the CAM criteria for GA on OCT B-scans.

Interestingly, Cleland et al. recently followed 70 eyes with GA using OCT with cRORA criteria for GA, as well as OCT with hyper-transmission criteria alone, FAF, CFP, and infrared imaging.[15] The authors found that the mean annual rate of GA growth was 1.6 mm^2 using the OCT scans with cRORA criteria, which is a bit faster than the rate found in our study. They found no significant difference between GA annotated using cRORA criteria and GA annotated using any of the other imaging modalities.

In our study, we found a significant correlation between focality at baseline and the rate of GA area progression. Similarly, Cleland et al.[15] evaluated GA progression using OCT annotation with cRORA criteria and found a significant correlation between multifocality at baseline and the rate of GA area progression. These findings are also consistent with the results of a meta-analysis of 3489 eyes, which included cases of atrophy imaged using CFP, FAF, and/or OCT.[3] The authors of this study suggested that this correlation between multifocality and GA area progression is related to the proportional increase in the total lesion perimeter being associated with a higher focality index.[3]

A recent work by this group (Shen et al.) demonstrated GA area growth rate to be strongly associated with baseline lesion perimeter. Importantly, they found GA perimeter-adjusted growth rate to be uncorrelated with focality, circularity, or total lesion size at baseline.[16]

A significant correlation between the lesion perimeter and GA area progression was demonstrated in our univariate analysis, but not in the multivariate analysis. Nonetheless, the findings of Shen et al. described above suggest that the greater baseline lesion perimeter correlated with multifocal GA lesions may be the cause of the associated higher rate of GA growth. This might be explained by the larger numbers of RPE cells that are exposed in the border of GA with greater lesion perimeter. This exposure at the border of healthy and atrophic retina may promote cellular events driving the atrophic process, such as apoptosis or immune-related cell death. However, further research is needed to better clarify the mechanisms explaining this finding.

We found a significant correlation between circularity at baseline and the rate of GA area progression on univariate analysis, but not in a multivariate model. Such a correlation was also reported by Cleland et al.[15] and in a previous study by Domalpally et al. involving 593 eyes measured using CFP.[17] In their report, Domalpally et al. suggested that low circularity may be associated with a larger lesion perimeter for a given lesion area[17]; it is worth mentioning that in a recent work by Shen et al., it was shown that the GA perimeter-adjusted growth rate is uncorrelated with circularity.[16] The greater lesion perimeter related with lower circularity may allow more RPE cells at the border of the lesion to be exposed to healthy retina. This may promote GA progression through the induction of certain cellular events, although this needs to be proven by further research. Although this explanation is plausible, our multivariate analysis showed that lesion perimeter was not correlated with GA area progression.

The average rate of square root area progression measured in our study (0.33 mm/year) is similar to previous measurements obtained with other imaging modalities, including CFP (0.30 mm/year),[17] FAF (0.31 mm/year),[8] and OCT without specifying cRORA criteria as the outcome (0.252 mm/year).[10] In agreement with the work of Domalpally et al.,[17] we found that both focality and circularity of the lesions were correlated with the square root area progression of GA on univariate analysis, but were not correlated on multivariate analysis. The possible explanation for this finding, as indicated for GA area progression, is the greater baseline perimeter of multifocal and noncircular lesions, involving more RPE cells at the border of the GA process.

In addition, previous studies have shown that using square root transformation makes the data more linear, decreasing the effect of baseline area on growth rate.[18] In concordance with this finding, the baseline area square root was not correlated with square root area progression in our work.

Interestingly, we found that the radial progression of GA toward the center was correlated with the minimum distance from the center at baseline (e.g. GA progressed more slowly toward the center when the lesion was closer to the center at baseline). This finding supports previous data showing initial preferential foveal sparing in select patients with dry AMD-related atrophy[19] and increased overall radial progression of atrophy with foveal sparing.[20] However, we found no published studies that specifically reported

a correlation between progression toward the center and minimum distance from the center at baseline. Nevertheless, both Curcio et al.[14] and Owsley et al.[15] previously speculated that the phenomenon of preferential foveal sparing may reflect the relatively higher resilience of cone cells against cell death compared rod cells.

In the present study, female sex was correlated with GA area progression rate on multivariate analysis and with radial progression towards the center only in the univariate analysis, but not in the multivariate analysis. In their 2018 meta-analysis, Fleckenstein et al. examined 6 studies that evaluated the putative correlation between sex and the rate of GA progression.[1] Although five of these six studies did not find a significant correlation, the study by Caire et al.[21] found that female sex was a risk factor for GA progression, with an adjusted odds ratio of 7.31. Patnaik et al. found that administration of exogenous estrogen to postmenopausal women had a protective effect against GA development.[22] The authors proposed that dysregulation of vascular and immune signaling pathways in the presence of lower levels of estrogen in postmenopausal women may be attenuated by exogenous estrogen replacement. This may suggest estrogen decline in postmenopausal women might promote GA development.

In our study, we used OCT scans to annotate GA based on the CAM criteria for classifying cRORA. In contrast, the majority of previous studies used FAF to detect and measure GA. However, the signal on FAF is susceptible to the effects of media opacities and optical aberrations. Moreover, quantifying absolute FAF signal intensity and comparing the results—either between subjects or within a given subject over time—is relatively complicated and remains a challenge in FAF imaging.[23] On the other hand, measuring GA using specific OCT criteria—as in our study—may provide more accurate results, as they rely on specific anatomic changes rather than signal intensity. In this respect, it is interesting to note that a recent study measuring the rate of GA growth over 12 months in 70 eyes found no difference between OCT with cRORA criteria and FAF imaging.[15] Nevertheless, studies including larger cohorts and longer follow-up times are needed in order to evaluate the difference between OCT and other imaging modalities, such as FAF, particularly given that increasing the accuracy of GA classification and GA measurements may provide an important tool for determining the inclusion of patients with GA in clinical trials and for measuring the rate of GA growth.

Our study has several limitations that warrant discussion. First, we included a relatively small patient cohort; thus, a larger cohort may have increased the precision of our calculations of progression and the resulting correlations. Second, we used only two graders in our study and the second grader annotated only 27% (14/52) of the scans independently; using additional independent graders may have reduced interobserver variability and increased the precision of our measurements. Third, the software that we developed for annotating GA in our study has not been independently validated. Fourth, the minimum diameter used to annotate GA lesions in our study was 200 microns and not 250 microns as specified by the CAM criteria.[11] Finally, the low scanning density (25 and 37 B-scans per cube scan) used for the imaging of some of the eyes may have a negative impact on the results due to insufficient imaging of the total area of GA.

On the other hand, a strength of our study is that the mean follow-up time was 24.7 months. Moreover, we quantitatively measured GA growth using OCT B-scans, thus assessing retinal anatomy during the annotation process.

In conclusion, we quantitatively measured the rate of GA area progression in patients with dry AMD using OCT B-scans rather than traditional FAF measurements, thus assessing retinal anatomy during the annotation process. We found that the rate of GA area progression was correlated with focality at baseline and female sex. In addition, we found that the radial rate of progression towards the center increased with increasing minimum distance between the lesion and the center.

Acknowledgments

Disclosure: **O. Shmueli**, None; **R. Yehuda**, None; **A. Szeskin**, None; **L. Joskowicz**, None; **J. Levy**, None

References

1. Fleckenstein M, Mitchell P, Freund KB, et al. The Progression of Geographic Atrophy Secondary to Age-Related Macular Degeneration. *Ophthalmology*. 2018;125:369–390.
2. Sadda SR, Guymer R, Holz FG, et al. Consensus Definition for Atrophy Associated with Age-Related Macular Degeneration on OCT: Classification of Atrophy Report 3. *Ophthalmology*. 2018;125:537–548.
3. Shen LL, Sun M, Grossetta Nardini HK, Del Priore L V. Progression of Unifocal versus Multifocal Geographic Atrophy in Age-Related

Macular Degeneration: A Systematic Review and Meta-analysis. *Ophthalmol Retin*. 2020;4:899–910.
4. Schmitz-Valckenberg S, Sahel JA, Danis R, et al. Natural History of Geographic Atrophy Progression Secondary to Age-Related Macular Degeneration (Geographic Atrophy Progression Study). *Ophthalmology*. 2016;123:361–368.
5. Szeskin A, Yehuda R, Shmueli O, Levy J JL. A column-based deep learning method for the detection and quantification of atrophy associated with AMD in OCT scans. *Med Image Anal*. 2021;72:102130.
6. Sayegh RG, Simader C, Scheschy U, et al. A systematic comparison of spectral-domain optical coherence tomography and fundus autofluorescence in patients with geographic atrophy. *Ophthalmology*. 2011;118:1844–1851.
7. Shen LL, Sun M, Khetpal S, et al. Topographic variation of the growth rate of geographic atrophy in nonexudative age-related macular degeneration: A Systematic Review and Meta-analysis. *Investig Ophthalmol Vis Sci*. 2020;61:2.
8. Pfau M, Lindner M, Goerdt L, et al. Prognostic value of shape-descriptive factors for the progression of geographic atrophy secondary to age-related macular degeneration. *Retina*. 2019;39:1527–1540.
9. Liefers B, Colijn JM, González-Gonzalo C, et al. A deep learning model for segmentation of geographic atrophy to study its long-term natural history. *Ophthalmology*. 2020;127:1086–1096.
10. Sayegh RG, Sacu S, Dunavölgyi R, et al. Geographic Atrophy and Foveal-Sparing Changes Related to Visual Acuity in Patients With Dry Age-Related Macular Degeneration Over Time. *Am J Ophthalmol*. 2017;179:118–128.
11. Sadda SR, Guymer R, Holz FG, et al. Consensus Definition for Atrophy Associated with Age-Related Macular Degeneration on OCT: Classification of Atrophy Report 3. *Ophthalmology*. 2018;125:537–548.
12. Simader C, Sayegh RG, Montuoro A, et al. A longitudinal comparison of spectral-domain optical coherence tomography and fundus autofluorescence in geographic atrophy. *Am J Ophthalmol*. 2014;158:557–566.
13. Zanzottera EC, Ach T, Huisingh C, et al. Visualizing retinal pigment epithelium phenotypes in the transition to atrophy in neovascular age-related macular degeneration. *Retina*. 2016;36(Suppl 1):S26–S39.
14. Rudolf M, Vogt SD, Curcio CA, et al. Histologic basis of variations in retinal pigment epithelium autofluorescence in eyes with geographic atrophy. *Ophthalmology*. 2013;120:821–828.
15. Cleland SC, Konda SM, Danis RP, et al. Quantification of Geographic Atrophy Using Spectral Domain OCT in Age-Related Macular Degeneration. *Ophthalmol Retin*. 2021;5:41–48.
16. Shen LL, Sun M, Ahluwalia A, et al. Geographic Atrophy Growth Is Strongly Related to Lesion Perimeter: Unifying Effects of Lesion Area, Number, and Circularity on Growth. *Ophthalmol Retina*. 2021;5:868–878.
17. Domalpally A, Danis RP, White J, et al. Circularity index as a risk factor for progression of geographic atrophy. *Ophthalmology*. 2013;120:2666–2671.
18. Feuer WJ, Yehoshua Z, Gregori G, et al. Square root transformation of geographic atrophy area measurements to eliminate dependence of growth rates on baseline lesion measurements: A reanalysis of age-related eye disease study report no. 26. *JAMA Ophthalmol*. 2013;131:110–111.
19. Sunness JS, Gonzalez-Baron J, Applegate CA, et al. Enlargement of atrophy and visual acuity loss in the geographic atrophy form of age-related macular degeneration. *Ophthalmology*. 1999;106:1768–1779.
20. Schmitz-Valckenberg S, Sahel JA, Danis R, et al. Natural History of Geographic Atrophy Progression Secondary to Age-Related Macular Degeneration (Geographic Atrophy Progression Study). *Ophthalmology*. 2016;123:361–368.
21. Caire J, Recalde S, Velazquez-Villoria A, et al. Growth of geographic atrophy on fundus autofluorescence and polymorphisms of CFH, CFB, C3, FHR1-3, and ARMS2 in age-related macular degeneration. *JAMA Ophthalmol*. 2014;132:528–534.
22. Patnaik JL, Lynch AM, Wagner BD, et al. Hormone Therapy as a Protective Factor for Age-Related Macular Degeneration. *Ophthalmic Epidemiol*. 2020;27:148–154.
23. Schmitz-Valckenberg S, Pfau M, Fleckenstein M, et al. Fundus autofluorescence imaging. *Prog Retin Eye Res*. 2021;81:100893.